

Ultrabroadband transmission measurements on waveguides of silicon-rich silicon dioxide

R. T. Neal, M. D. C. Charlton,^{a)} and G. J. Parker^{a)}

Department of Electronics and Computer Science, University of Southampton, Southampton SO17 1BJ, United Kingdom

C. E. Finlayson,^{b)} M. C. Netti,^{a)} and J. J. Baumberg^{a)}

Department of Physics and Astronomy, University of Southampton, Southampton SO17 1BJ, United Kingdom

(Received 17 July 2003; accepted 8 October 2003)

We report ultrabroadband measurements on waveguides of photoluminescent silicon-rich silicon dioxide produced by plasma enhanced chemical vapor deposition. Material absorption below 700 nm and waveguide loss above 1300 nm leave a broad spectral region of good transmission properties, which overlaps with the photoluminescence spectrum of the core material. Proposed mechanisms for the material absorption and photoluminescence are discussed based on our findings.

© 2003 American Institute of Physics. [DOI: 10.1063/1.1631065]

The use of silicon as the basis of the microelectronics industry has led to it being the best characterized and understood material in the world. Silicon is so widely used primarily because of silicon dioxide's excellent properties as an electrical insulator, although the relatively inexpensive nature of the material must also be considered an incentive.¹ While bulk silicon possesses good electrical properties, it is an indirect band gap material, resulting in very low band edge luminescence efficiency.²

The motivation for silicon light emitting devices is so great that many methods have been developed to attempt to overcome this problem. These include doping with carbon,³ implantation with rare earth elements,⁴ dislocation engineering,⁵ and recently, reverse solar cells.⁶ Since the discovery by Canham in 1990 of strong photoluminescence from porous silicon,⁷ there has been strong interest in light emitting nanoscale silicon structures. This was further fuelled by an article by Pavesi⁸ in which optical gain was reported in waveguides of silicon nanocrystals implanted into silicon dioxide. Much work has continued on silicon nanocrystals, with ion implantation,⁹ sputtering,¹⁰ and plasma enhanced chemical vapor deposition (PECVD) being the favored fabrication techniques. Following initial work by Iacona *et al.*¹¹ on the growth of silicon nanocrystals, we have now succeeded in fabricating strongly luminescent planar optical waveguides based on nanocrystalline silicon material.

Any optical circuit to be made from luminescent silicon nanocrystals will have the waveguide as its fundamental element. However, there are no broadband measurements available in the current research literature setting out the critical transmission properties of waveguides of silicon-rich silicon dioxide (SRSO). These properties, essential to the fabrication of integrated circuits in SRSO, are reported in this letter. Ultrabroadband transmission measurements have been carried out which present the transmission properties of

waveguides of PECVD SRSO for wavelengths from approximately 600 to 1600 nm.

To form a waveguide, silicon wafers were thermally oxidized to a thickness of over 2 μm . A layer of silicon-rich silicon dioxide 450-nm-thick was deposited upon the thermally grown silicon dioxide by PECVD. The level of silicon incorporation in the layer was controlled by varying the ratio of the composite gases, SiH_4 and N_2O . To complete the structure, a cladding layer of 200 nm standard PECVD silicon dioxide was deposited on top (shown in the inset of Fig. 2). To activate the photoluminescent properties of the SRSO, some of the waveguides were annealed at 1150 °C for durations ranging from 30 min to 6 h. Table I shows how the refractive index and layer thickness (measured by ellipsometry at 633 nm for separate thin film calibration samples) of the core layer of each waveguide changed with the activation anneal. The postanneal refractive index was constant for all durations of anneal.

In order to determine the photoluminescent properties of the samples, a 30 mW beam from an argon ion laser ($\lambda=514$ nm) was focused into a spot of approximately 20 μm diameter at the edge of the waveguide and used to photoexcite the SRSO. This power density was used because the active layer is so thin at normal incidence, and the absorbing Si nanoparticles fill <1% of the volume [see Fig. 4(a)], leading to inefficient optical pumping in this geometry. The resulting photoluminescence was collected at the edge of the waveguide and collimated using a 90 \times microscope objective. This light was then coupled into a spectrometer. Although there was little difference between the TE and TM polarized luminescence spectra, all reported measurements were carried out in the TE polarization.

Results for the photoluminescence measurements carried out are shown in Fig. 1. The spectrometer used was a nitrogen-cooled silicon charge coupled device (CCD) detector, giving a spectral resolution of a few nanometers with an effective wavelength range of 450 nm–1.1 μm . Figure 1(a) demonstrates how the peak intensity of the luminescence shifts to the longer wavelengths with increasing the silicon

^{a)}Also at: Mesophotonics Ltd., 2 Venture Rd., Chilworth Science Park, Southampton SO16 7NP, United Kingdom.

^{b)}Electronic mail: cef@phys.soton.ac.uk

TABLE I. Key parameters for the SRSO waveguides used in these experiments, both before and after the annealing stage. The refractive index and film thickness values were measured by ellipsometry.

Wafer type	Ratio (SiH ₄ N ₂ O)	<i>n</i> (before)	Thickness (before, Å)	Annealing time (h)	<i>n</i> (after)	Thickness (after, Å)
A	12	1.605	4345	0.5,1,3,6	1.685	5720
B	9	1.575	4524	0.5,1,3,6	1.576	3850
C	6	1.547	4621	0.5,1,3,6	1.528	4047

incorporation in the SRSO. We also found clear evidence that as the anneal time increases, so does the intensity of the luminescence from the SRSO. This is shown in Fig. 1(b) for wafer type “A.” These results would appear to be in contrast with those reported by Brongersma *et al.*¹²

Waveguide transmission measurements were carried out using an ultrabroadband continuum generated from a nonlinear photonic crystal “holey” fiber. The fiber was pumped using the 150 fs, $\lambda=1100$ nm idler output from a pulsed optical parametric amplifier derived from a regeneratively amplified Ti:sapphire femtosecond-pulsed laser. The resulting supercontinuum was observed to range from around 600 to 1600 nm in wavelength and was tightly focused into the core layers of the SRSO waveguides. The transmitted light was measured using both a peltier-cooled Si CCD (500–1100 nm) and an InGaAs infrared detector (900–1800 nm), in order to cover the full spectral range. A reference beam was routed around the waveguide to allow the relative transmittance spectra to be accurately derived.

Figure 2 shows the spectra for transmission through a waveguide of wafer type “B” (core thickness 385 nm) which has been annealed for 1 h (solid line), transmission through an unannealed waveguide (short dashed line) and the photoluminescence, all for the same waveguide sample. It may be seen that the unannealed waveguide has much better transmission properties in the visible portion of the spectrum, although it exhibits no photoluminescence. It is also clear that the annealed waveguides have improved waveguide transmission in the IR portion of the spectrum. The photoluminescence of the sample has also been appended to Fig. 2 to illustrate how closely the absorption losses at shorter wavelengths matches the onset of the photoluminescence.

Focusing upon the visible and near IR portion of the spectrum, we observe that the wavelength at which the an-

nealed waveguides begin to guide is not dependent upon either the duration of the anneal [Fig. 3(a)] or upon the silicon incorporation of the sample [Fig. 3(b)]. We attribute the waveguide losses below 700 nm to optical absorption by silicon nanocrystals, which have formed during the thermal anneal. Figure 4(a) shows an absorption model for a silicon dioxide waveguide¹³ with a silicon incorporation of 0.04% plotted with our experimental results. As no silicon could possibly have been added postdeposition, it is interesting to note that the silicon only becomes actively absorbing after the anneal stage. This is consistent with the occurrence of characteristic silicon nanocrystal photoluminescence only in those samples which have been annealed. We believe that the relatively broad material absorption band below 700 nm illustrates the cluster size range, and the invariant edge at 700 nm suggests a band gap energy of 1.77 eV for the largest optically active silicon nanocrystals. This is in agreement with work done by Ma *et al.* in 1999,¹⁴ who reported a similar consistent absorption edge between 1.65 and 1.8 eV, corresponding to 690–776 nm.

We also believe that the improved waveguide transmission in the IR after annealing is as a result of the raised refractive index of the core layer. Figure 4(b) shows calculations of how the effective refractive index of the waveguide core layer varies as a function of wavelength.¹⁵ As all samples measured exhibited similar IR losses (shown for wafer type B in Fig. 2), it is not probable that waveguide cutoff is the sole loss mechanism. We would expect that absorption losses in the SiO₂ cladding layers will cause attenuation of the waveguide modes in the core layer. It is noted that the losses above 1300 nm are very similar to the characteristic IR absorption losses, which are among the major loss factors in SiO₂ optical fibers.¹⁶

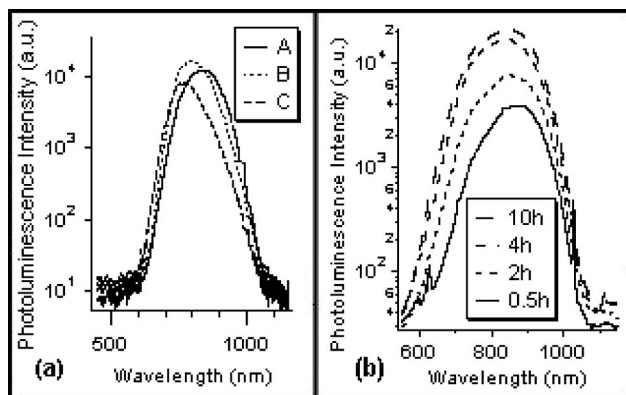


FIG. 1. Photoluminescence spectra for waveguides of SRSO showing (a) the redshift in peak intensity wavelength with increasing silicon incorporation into the SRSO core layer, and (b) increasing photoluminescence intensity as a function of anneal duration.

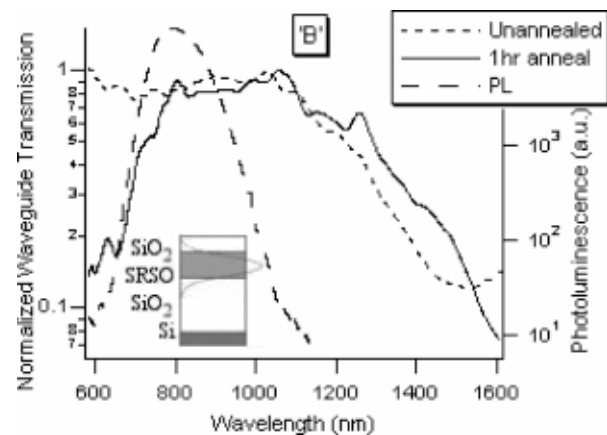


FIG. 2. Full ultrabroadband transmission spectra for both annealed and unannealed SRSO waveguide samples together with the photoluminescence spectrum of the core material. The inset shows a schematic diagram of the waveguide structure.

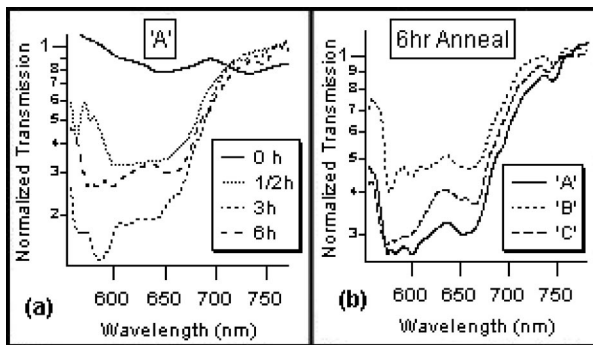


FIG. 3. Visible transmission spectra for waveguides of SRSO around the onset wavelength of nanocrystal absorption which (a) is invariant with respect to anneal duration, and (b) is invariant with respect to silicon incorporation in the core layer.

Despite strong absorption below 700 nm and above 1300 nm, waveguides of luminescent SRSO are efficient waveguides for the near IR portion of the electromagnetic spectrum. This is especially pertinent for the 700–1000 nm portion of the spectrum, in which SRSO generates photoluminescence. The waveguide will, however, reabsorb the higher energy portion of the photoluminescence spectrum as it passes through the material.

While the optical absorption of the material is attributed to band gap absorption in delocalized states of the silicon nanocrystals, the photoluminescence clearly originates from a different mechanism. This is attributed to radiative recombination from interface states between the silicon nanocrystals and the surrounding SiO₂ matrix.¹⁷ While the shift in the

wavelength of peak intensity may be considered a result of different cluster size distributions as the silicon incorporation of the SRSO changes, we believe the increase in photoluminescence intensity as a function of anneal time is either due to the continued formation of radiative interface states or to the annealing out of nonradiative recombination pathways associated with defects formed during the amorphous PECVD process. Detailed luminescence lifetime measurements may in the future allow this issue to be clarified.

In conclusion, waveguides of luminescent (annealed) and nonluminescent (unannealed) SRSO were fabricated using PECVD. Unannealed waveguides exhibited good transmission qualities throughout the visible spectrum, while annealed waveguides were absorbing below 700 nm. The onset wavelength for this absorption was invariant with changes to the anneal time and silicon incorporation in the waveguide core layer. This demonstrates that waveguides of SRSO exhibit favorable optical properties for the portion of the electromagnetic spectrum in which the core material is photoluminescent. This work prepares the way for integrated devices incorporating luminescent SRSO waveguides as a fundamental component.

¹S. M. Sze, *Semiconductor Devices—Physics and Technology* (Wiley, New York, 1985).

²J. R. Haynes and W. C. Westphal, *Phys. Rev.* **101**, 1676 (1956).

³L. T. Canham, K. G. Barraclough, and D. J. Robbins, *Appl. Phys. Lett.* **51**, 1509 (1987).

⁴H. Ennen, J. Schneider, G. Pomrenke, and A. Axmann, *Appl. Phys. Lett.* **43**, 943 (1983).

⁵W. L. Ng, M. A. Lourenço, R. M. Gwilliam, S. Ledain, G. Sho, and K. P. Homewood, *Nature (London)* **410**, 192 (2001).

⁶T. Trupke, J. Zhao, A. Wang, R. Corkish, and M. A. Green, *Appl. Phys. Lett.* **82**, 2996 (2003).

⁷L. T. Canham, *Appl. Phys. Lett.* **57**, 1046 (1990).

⁸L. Pavesi, L. Dal Negro, C. Mazzoleni, G. Franzo, and F. Priolo, *Nature (London)* **408**, 440 (2000).

⁹T. Shimizu-Iwayama, N. Kurumado, D. Hole, and P. Townsend, *J. Appl. Phys.* **83**, 6018 (1998).

¹⁰O. Hanaizumi, K. Ono, and Y. Ogawa, *Appl. Phys. Lett.* **82**, 538 (2003).

¹¹F. Iacona, G. Franzo, and C. Spinella, *J. Appl. Phys.* **87**, 1295 (2000).

¹²M. L. Brongersma, A. Polman, K. S. Min, E. Boer, and T. Tambo, *Appl. Phys. Lett.* **72**, 2577 (1998).

¹³K. Rajkanan, R. Singh, and J. Shewchun, *Solid-State Electron.* **22**, 793 (1979).

¹⁴Z. Ma, X. Liao, G. Kong, and J. Chu, *Appl. Phys. Lett.* **75**, 1857 (1999).

¹⁵K. Okamoto, *Fundamentals of Optical Waveguides* (Academic, San Diego, 2000).

¹⁶A. Ghatak and K. Thyagarajan, *Introduction to Fibre Optics* (Cambridge University Press, Cambridge, 1998).

¹⁷L. Dal Negro, M. Cazzanelli, L. Pavesi, S. Ossicini, D. Pacifici, G. Franzo, F. Priolo, and F. Iacona, *Appl. Phys. Lett.* **82**, 4636 (2003).

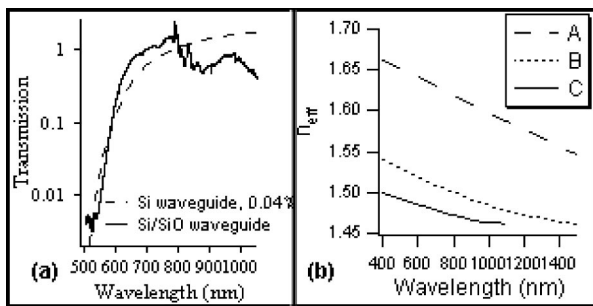


FIG. 4. Models for (a) transmission of a bulk silicon dioxide waveguide with a 0.04% incorporation of silicon, plotted with experimental results for a waveguide of wafer type A and (b) the refractive index of each waveguide sample core illustrating cutoff around 1100 nm for wafer type C and beyond 1500 nm for types A and B.